REPORT NO. 93
JULY, 1955.

THE COLLEGE OF AERONAUTICS
CRANFIELD

Measurement of the Derivative z_w for oscillating Wings in Cascade

-by-

Ronald D. Milne, B.Sc., D.C.Ae.,
and
Frank G. Willox, B.Sc., D.C.Ae.

SUMMARY

Experimental results are reported of the damping derivative z_w for rigid rectangular wings of various aspect ratios in cascades having gap-chord ratios of 2, 1, $\frac{1}{2}$, 1/3, 1/4. The results show fair agreement with two-dimensional theory. The ranges of Reynolds numbers and frequency parameters were 0.8 to 2.5 x 10^5 and 0.1 to 0.45 respectively.

The results show a strong dependence on Reynolds number which increases with decrease in gap-chord ratio. This effect was eliminated by transition fixation by wires placed at suitable positions downstream of the wing leading edge.

This report was submitted in 1954 as a part requirement for the award of the Diploma of the College of Aeronautics.

MEP

CONTENTS

LIST OF SYMBOLS

f_N	Natural frequency of oscillation
f_R	Resonant frequency of oscillation
$\bar{l}$	Exciting amplitude
p_s	Static pressure
S	Wing area
V	Windspeed
Z	Aerodynamic force normal to planform
$\bar{z}_R$	Amplitude of resonant oscillation of wing
$Z_w = \frac{\partial Z}{\partial w}$	Aerodynamic damping derivative
$z_w = \frac{Z_w}{\rho V S}$	Non-dimensional damping derivative
λ	Spring stiffness
$\omega = \frac{2\pi f_R c}{V}$	Non-dimensional frequency parameter

---

1. Introduction

The purpose of this experiment was to measure the damping derivative z_w for rectangular wings in cascade oscillating with simple harmonic motion.

Work has already been done to determine the derivative z_w for isolated rectangular and sweptback wings (refs. 1,3 and 4) and for rectangular wings in cascade (ref. 2).

The results of ref. 2 are inconclusive for gap-chord ratios of 1 and less owing to a Reynolds number effect which gives rise to very erratic results.

It was found in ref. 6 that adjacent aerofoils in cascade oscillated approximately 180° out of phase when fluttering. They may therefore be regarded as images of each other in a rigid plane boundary between them. These conditions may be represented

experimentally by an aerofoil oscillating between two parallel plates. In theory these plates should be of infinite length but on approximation to the true conditions can be obtained with plates of finite length.

Experiments along the same lines as those of ref. 2 were made at gap-chord ratios of $\frac{1}{2}$ and 1/3, but on the basis of some preliminary investigations, transition wires were added to aerofoils and image plates in an attempt to fix transition and thus eliminate Reynolds number effects.

2. Apparatus

2.1. General

The tunnel and oscillating rig were basically those used for the experiments of reference 1 with the addition of two parallel plates in the working section as shown in figure 1.

Three rectangular wing models were used all of 3in. constant chord and having aspect ratios of 5, 4 and 3. The aerofoil section was NACA 0010.

Transition wires were fitted to the aerofoils and to the plates as described in para. 5.1.

The frequency of oscillation of the rig was measured by means of an electrical tachometer which had been calibrated against a Hasler revolution counter connected directly to the eccentric shaft (figs. 2 and 3).

The forcing amplitude was measured by means of a dial gauge reading directly the stroke of the eccentric. The amplitude at resonance was measured by observing the deflection of a beam of light shining on a small mirror attached to the rig. The reflected image could be measured to within 0.01in. displacement.

Two sets of springs were used and they were adjusted so that the spring tension was the same with each set of springs in position on the rig.

The stiffnesses of the springs were measured by hanging weights from the springs and measuring the deflections with a pair of Vernier Calipers. The two sets are referred to as (A) and (B) and have the following stiffnesses.-

$$\text{A springs} \begin{cases} A_1 - 210 \text{ lb./ft.} \\ A_2 - 230 \text{ lb./ft.} \end{cases}$$

B springs $\begin{cases} B_1 - 85.5 \text{ lb./ft.} \\ B_2 - 80.5 \text{ lb./ft.} \end{cases}$

2.2 Measurement of wind speed

The wind speed was measured by a Prandtl Manometer connected to a static hole in the roof of the tunnel. During the tests two such static holes were used owing to the blockage of the normal hole for gap-chord ratios less than $\frac{1}{2}$. (See fig. 4).

The normal static hole is situated 1.3/8in. off the tunnel axis (see fig. 4). Since this static hole could not be used for the tests at $\frac{1}{2}$ and 1/3 gap-chord ratio another static hole was chosen on the tunnel axis (hole No. 4, fig. 4).

Typical calibration curves for these two static holes are shown in figs. 5 and 6. These curves were obtained by comparing the manometer reading with the true velocity as read by a pitot tube, in the working section between the plates at the model position.

The static pressure distribution along the tunnel axis is shown in fig. 7 for the 1/3 and $\frac{1}{2}$ gap-chord ratio configurations.

The pitot tube used for the calibrations was also traversed between the plates at the model position. It was found that the velocity was constant between the plates.

2.3 The measurement of z_w

The method used for the measurement of z_w is described in detail in reference 1.

For a given value of the exciting amplitude ($\bar{l}$) readings were taken of the resonant frequency (f_R) and resonant amplitude ($\bar{z}_R$) at a wind speed (V).

2.4 Reynolds number and frequency parameter

The range of Reynolds number (Vc/ν) used in these tests was 0.8×10^5 to 2.5×10^5.

The range of frequency parameter $\omega = \frac{2\pi f_R c}{V}$ was 0.1 to 0.45 where f_R is the resonant frequency
c is the aerofoil chord
V is the wind speed.

3. Details of Tests

3.1 Preliminary Investigations

The data of ref. 2 for a gap-chord ratio of $\frac{1}{2}$, indicated that considerable scatter of the results was obtained which was found to be due to a Reynolds number effect due presumably to transition movements on both plates and aerofoils.

It was therefore decided to make a preliminary qualitative investigation designed to show the mean transition position under oscillatory conditions. A sublimation technique was employed. The aerofoil was sprayed with a Napthalene-Petroleum Ether - Toluene mixture. For these tests a tunnel speed of 160 f.p.s. was used.

The results obtained were not conclusive but on an average it appeared that transition occurred at about 60 per cent chord but no two tests gave identical results.

On the basis of this information it was decided to fit transition wires at 25 per cent chord on the aerofoil. The size of wire used was determined from the accepted relation for steady flow $Vd/\nu > 600$. Since the results of reference 2 became irregular in the speed range 70-100 f.p.s., a wire diameter of 18 thousandths of an inch was used.

It was subsequently found (see para. 5.1) that this diameter was insufficient and rather than increase wire diameter, the wires on the aerofoils were brought forward to 10 per cent chord and wires of the same diameter (18 thou.in.) were fixed on the plates at 10 per cent of the plate chord.

3.2 Main Test Procedure

It was noted in ref. 2 that variation of resonant amplitude did not appreciably affect the value of z_w. This was substantiated by a preliminary test at a gap-chord ratio of 1 in which curves were obtained of $\bar{z}_R/l$ against $1/V$ (fig. 8) both keeping resonant amplitude constant and forcing amplitude constant.

It was therefore decided to keep the exciting amplitude constant and allow the resonant amplitude to vary. Furthermore three exciting amplitudes were used where possible; the largest being limited by the aerofoil banging against the plates and the smallest limited by the amplitude which could be measured reasonably accurately by the technique used.

After experience gained in initial tests the following values of exciting amplitude were decided upon.-

.0300in., .0150in., .0075in.

All the main tests were performed with transition wires of 18 thou.in. diameter on aerofoils and plates at 10 per cent chord. Tests were performed for each wing with each set of springs at gap-chord ratios of $\frac{1}{2}$, 1/3 and 1/4 using selected values of the chosen exciting amplitudes.

Before commencing tests it was checked that the aerofoil incidence was zero by running up the tunnel with the forcing rig stationary, and noting whether the model was displaced from the central position. If this was the case the incidence was corrected by 'trial and error'.

To avoid 'banging', the aerofoil was pulled against the plates and the amplitude set on the scale. The tunnel was then run at a reasonably high speed, say 80 f.p.s., and the frequency brought to resonance when it could be seen from the amplitude trace whether the aerofoil was 'banging' or not. If it was not 'banging' the tunnel speed was decreased until either the aerofoil was 'banging' or minimum tunnel speed was reached.

For any particular tunnel speed the resonant amplitude was most accurately and easily measured by going slowly through the resonant condition in both directions several times.

Graphs of $\bar{z}_R/l$ against $1/V$ were plotted* concurrently with the test to ensure that enough readings were being taken to give sufficient accuracy. To allow for hysteresis effects several check readings were taken while decreasing tunnel speed, the main set of readings having been obtained while increasing tunnel speed.

4. Results

4.1 Velocity Calibrations

Velocity calibration curves for $\frac{1}{2}$ and 1/3 gap-chord ratios are shown in figs. 5 and 6.

The distribution of static pressure along the tunnel axis for $\frac{1}{2}$ and 1/3 gap-chord ratios is shown in fig. 7. These curves are the averages of distributions corresponding to a series of tunnel speeds throughout the speed range used in the tests.

---

* It was found in reference 1 that $\bar{z}_R/l$ was approximately linear with $1/V$.

4.2 Preliminary Tests

4.2.1 Gap-chord ratio of 1

Fig. 8 shows curves of $\bar{z}_R/l$ against $1/V$ for Wing III with transition wires of 18 thou.in. diameter on aerofoil and plates both for fixed resonant and fixed exciting amplitudes.

4.2.2 Gap-chord ratio of $\frac{1}{2}$

Figs. 9 and 10 show curves of $\bar{z}_R/l$ against $1/V$ for Wings II and III with no transition wires on plates or aerofoils, and fig. 11 corresponding results for Wing III with transition wires on aerofoil only at 25 per cent chord.

4.2.3 Gap-chord ratio of 1/3

Figs. 12 and 13 show curves of $\bar{z}_R/l$ against $1/V$ for Wings I and II with no transition wires and fig. 14 shows Wing II with transition wires of 34 thou.in. diameter on aerofoil and plates at 10 per cent chord.

4.2.4 Gap-chord ratio of 1/4

A few results were obtained for a gap-chord ratio of 0.25 for Wings I, II and III with 0.018in. diameter transition wires fixed at 10 per cent chord. The results did not give a linear relation between $\bar{z}_R/l$ and $1/V$ and it was suspected that the diameter of the transition wires was insufficient to fix transition in this case.

4.3 Main Tests

4.3.1 $\bar{z}_R/l$ against $1/V$ curves

In figs. 15-20 are drawn curves of $\bar{z}_R/l$ against $1/V$ for $\frac{1}{2}$ and 1/3 gap-chord ratios, for Wings I, II and III with transition wires of 18 thou.in. diameter at 10 per cent chord on the aerofoils and plates.

4.3.2 z_w against a curves

From the curves of figs. 15-20, z_w is calculated according to the formula

$$z_w = \frac{-1}{\rho V S}\left[\frac{\lambda \bar{l}}{2\pi \bar{z}_R f_N}\right] \qquad \text{(ref. 1)}$$

This assumes that frictional damping in the oscillating rig has been neglected. This is justified since it is shown in ref. 3, Appendix I, that μ is only significant when the resonant amplitude is large ($\bar{z}_R > 0.3$in.) Throughout these tests the resonant amplitude was always smaller than 0.3in.

It is shown in ref. 2, para. 3.4, that the natural frequency of the system, f_N, may be taken equal to the resonant (forced) frequency, f_R, within the limits of experimental error. However, in all cases the results were evaluated using the measured resonant frequency.

Curves of (z_w) against ω are shown in figs. 21 - 26.

4.3.3 Summary of Results for $\omega = 0.2$

In fig. 27 are shown curves of $(-z_w)$ against inverse of aspect ratio for constant gap-chord ratio and these are extrapolated to give values of $(-z_w)$ for infinite aspect ratio for gap-chord ratios of ∞, 2, $\frac{1}{2}$ and 1/3.

The curve for gap-chord ratio of 2 is obtained from ref. 2 and the curve for infinite gap-chord ratio from ref. 5.

In fig. 28 a curve for each wing is given showing the variation of $(-z_w)$ with gap-chord ratio.

In fig. 29 the values of $(-z_w)$ for infinite aspect ratio as obtained from fig. 26 are compared with the theoretical, two-dimensional values obtained from ref. 6 for low gap-chord ratios and from ref. 5 for infinite gap-chord ratio.

5. Discussion of Results

5.1 Preliminary Tests

Before eliminating any Reynolds number effect by fitting transition wires it was felt desirable to try and reproduce the results obtained in ref. 2, figs. 11 and 12 for a gap-chord ratio of $\frac{1}{2}$. Tests were therefore done with no transition wires and the $\bar{z}_R/l$ against $1/V$ curves are shown in figs. 9, 10, 12 and 13 for gap-chord ratios of $\frac{1}{2}$ and 1/3.

It was found impossible to reproduce exactly the results of figs 11 and 12, ref. 2.

Figs. 12 and 13 for gap-chord ratio of 1/3 show curves of the same form as fig. 9 but the trend is more sharply defined.

This suggests that the irregular curves of $\bar{z}_R/l$ against $1/V$ which are associated with a Reynolds number effect are also a function of gap-chord ratio.

It was felt that if the Reynolds number effect could be completely eliminated the curves of $\bar{z}_R/l \sim 1/V$ obtained would resemble those of figs. 2 - 6, ref. 1 which are almost linear.

Fig. 11 shows that when 18 thou.in. diameter wires were fitted at 25 per cent chord on Wing III a partial improvement of the results was obtained but it was not until the wires were moved forward to 10 per cent chord on the aerofoil and similar wires were fitted at 10 per cent chord on the plates that the desired result was obtained (see figs. 15, 16, and 17).

The fact that it was found impossible to reproduce the results of figs. 11 and 12, ref. 2, suggests that the inconsistencies shown in these results can not be wholly explained by Reynolds number effect. From experience gained using the apparatus the authors suggest that lack of rigidity in the model supports could have caused the otherwise unexplained irregularities in the previous results.

Conditions without transition wires were very unsteady and it was difficult to obtain accurate readings of resonant amplitude owing to irregular movements of the centre of oscillation of the aerofoil. In contrast, tests performed with transition wires on aerofoils and plates could be carried through in a straightforward manner and the results reproduced at will.

It was found that, for any one set of springs, the curves of $\bar{z}_R/l \sim 1/V$ for different forcing amplitudes were distinctly separated when no transition wires were present, while the corresponding curves for transition wires in position were practically coincident (cf. figs. 10 and 17). In addition test conditions were found to be much steadier when the stronger set of springs (A) were used.

5.2 Main Tests

5.2.1 Curves of $\bar{z}_R/l$ against $1/V$

Comparing figs. 15 - 17 with figs. 2 - 6 of ref. 1 it will be seen that using different sets of springs has the same general effect on the value of $\bar{z}_R/l$.

The curves for a gap-chord ratio of 1/3, figs. 18 - 20, are similar to those at a gap-chord ratio of $\frac{1}{2}$ (figs. 15 - 17) but at low tunnel speeds the curves change slope. It was thought that this effect was again due to Reynolds number.

In order to verify this tests were performed using wires of 34 thou.in. diameter at 10 per cent chord on the aerofoil (Wing II) and plates, and the results obtained are shown in fig. 14. These curves are now very regular and conditions during the test were found to be even steadier than those associated with the 18 thou.in. diameter wires on aerofoil and plates.* This indicates that the Reynolds number effect increases with decrease in gap-chord ratio.

5.2.2 Variation of z_w with ω

The curves of $(-z_w) \sim \omega$ at a gap-chord ratio of $\frac{1}{2}$ (figs. 21 - 23) are similar to those obtained for a gap-chord ratio of 2 in ref. 2 (figs. 15, 16 and 17) and in ref. 1 for isolated rectangular wings (figs. 7 and 8).

According to theory there should be a unique curve for any one wing but this is not borne out by the present results or the results of refs. 1 and 2. It has been suggested in ref. 1, para. 8 that this discrepancy between theory and practice is due entirely to experimental error. This is borne out, to some extent in the present tests, since the curves at a gap-chord ratio of $\frac{1}{2}$ (figs. 21 - 23) for different springs and different forcing amplitudes are not displaced far from each other and there does not appear to be any definite trend in the relative displacements of the curves for any particular wing.

The experimental curves for $(-z_w) \sim \omega$ at a gap-chord ratio of 1/3 (figs. 24 - 26) appear to be valid only over a limited range of frequency parameter and this, as remarked in para. 5.1, is due to the Reynolds number effect reasserting itself at low tunnel speeds. (It can be seen from fig. 14 that more consistent results would have been obtained if 34 thou.in. diameter transition wires had been used).

Although the effect of changing exciting amplitude is still small the relative displacements of curves for different springs appear to be much larger than for a gap-chord ratio of $\frac{1}{2}$.

In order to demonstrate that the sudden increase in z_w for the A and B springs occurs at the same value of the Reynolds number, let us assume that a Reynolds number effect takes place at a speed V_1, such that for $V > V_1$ the variation of z_w with ω is small, but for $V < V_1$ there is a sudden increase in the value of z_w. The resonant frequency using springs B is in the region of 7.6 c.p.s. and with springs A is in the region of 13 c.p.s. Thus the values of ω corresponding to the sudden

---

* All the tests at 1/3 gap-chord ratio had been completed, using a transition wire 0.018in. diameter at 10 per cent chord on both the aerofoils and plates, before the tests using a wire 0.034in. diameter were performed.

increase in z_w (for a fixed speed V_1) will be in the ratio,

$$\frac{(\omega)_{B\ \text{springs}}}{(\omega)_{A\ \text{springs}}} \simeq \frac{7.6}{13} = \frac{1}{1.7} \quad .$$

Reference to figs. 24 - 26 shows that this is the case and that there does exist a critical speed V_1 at which the flow changes character. A similar effect was observed in ref. 2 where, by plotting z_w against $1/V$, curves for different springs were made to coincide approximately (fig. 17, ref. 2).

It is the different relative positions of the rapid increase in z_w for the two sets of springs which makes the curves appear to be displaced. Results obtained using larger wires would probably eliminate the rapid rise and would give results similar to those for a gap-chord ratio of $\frac{1}{2}$ (figs. 21-23).

5.2.3 Final Results

It is necessary to fix on a value of a before the variation of z_w with aspect ratio and gap-chord ratio can be presented. A value of $\omega = 0.2$ was taken since it lies in the middle of the range considered and in the case of gap-chord ratio of 1/3 the curves at $\omega = 0.2$ are above the 'critical speed', V_1, for both sets of springs, and therefore not in the range affected by Reynolds number.

Results for $a = 0.2$ should be typical of those for ω general (over the range considered), since, when Reynolds number effect is eliminated, the dependence of z_w on ω is small.

In order to compare the results of the present tests with those derived on the basis of two-dimensional theory in ref. 6 it was necessary to estimate the value of z_w corresponding to infinite aspect ratio at each gap-chord ratio. As a basis for the extrapolation the results of ref. 5 for infinite gap-chord ratio and rectangular aerofoils were plotted and it was found (fig. 27) that the extrapolation was linear. Accordingly, mean straight lines were drawn through the groups of points taken from the curves of figs. 21 - 26, for each spring and exciting amplitudes and produced to meet the $(-z_w)$ axis (fig. 27).

The set of results seems to be consistent; the rate of increase of z_w with aspect ratio being more rapid at smaller gap-chord ratios. This is brought out more clearly in fig. 28.

The results of ref. 2 for a gap-chord ratio of 1 were inconsistent with the curves of fig. 27 and so were omitted.

Fig. 28 shows that the variation of z_w with gap-chord ratio is similar for all the aspect ratios considered. As gap-chord ratio decreases, z_w increases and for gap-chord ratios less than 0.5 the rate of increase is very rapid.

It is improbable that $(-z_w)$ will continue to increase as indicated in fig. 28 and this was confirmed in the preliminary tests made at a gap-chord ratio of 1/4.*

It is shown in fig. 29 that for gap-chord ratios in the range 1/3 to 1/2 very good agreement is obtained between theory and experiment. The theoretical curve was derived from approximate formulae given in ref. 6 which only apply for small gap-chord ratios (≤ 1).

5.3. Air-resonance condition

It is pointed out in ref. 7 that for aerofoils oscillating between walls in a compressible flow a transverse resonance phenomenon can exist which can greatly change the nature of the flow. This is due to the fact that in a compressible fluid there is a definite time lag between a disturbance initiated at one point and its effect at another. Under certain conditions this phase lag can give rise to a resonant condition (of the air) which involves large corrections.

Woolston and Runyan (ref. 7) give a curve relating the critical frequency at which the above resonant condition occurs to tunnel height and Mach number. For the Mach number range used throughout the present tests this critical frequency is practically constant and furthermore this frequency is much higher than either of the resonant frequencies associated with springs A and B (13 and 7.6 c.p.s. respectively).

6. Acknowledgements

The authors with to acknowledge the assistance given by Mr. G.M. Lilley and Mr. K.D. Harris throughout this investigation. Mr. S.H. Lilley was responsible for improving the accuracy of the apparatus, Mr. S. Clarke made the plates and Mr. C.D. Bruce the wooden aerofoils.

Acknowledgements are also due to Messrs. B.S. Campion and E.G. Seacy for use of unpublished information.

---

* As noted above the results at a gap-chord ratio of 1/4 probably suffer from lack of transition fixation. It is for this reason that these results are not reported.

7. Conclusions

1. z_w has been measured, using a forced oscillation technique, on rigid rectangular wings oscillating between parallel plates. The results are applicable to aerofoils in cascade when adjacent blades are oscillating in antiphase.

2. Attention is drawn to the large Reynolds number effect on the values of z_w. This effect, which increases with decrease in the gap-chord ratio, is associated with the movement of the transition region on the aerofoils and side plates. Tests show that the Reynolds number effect can be eliminated by fixing a large enough transition wire to the aerofoil near the leading edge of both the aerofoils and side plates.

3. When the Reynolds number effect is eliminated the dependence of z_w on the frequency parameter is small. The range of frequency parameters used in the tests was 0.1 to 0.45 and the range of Reynolds number was 0.8×10^5 to 2.5×10^5.

4. The variation of z_w with gap-chord ratio was found for aerofoils of aspect ratios 5, 4 and 3 at gap-chord ratios of 2, 1, $\frac{1}{2}$, 1/3 and 1/4. The results, when extrapolated to infinite aspect ratio, showed fair agreement with the approximate theoretical values obtained in reference 6. The large increase in the value of z_w with decrease in gap-chord ratio, as predicted by theory, is shown to be true for values of gap-chord ratio above 1/3. At smaller values of gap-chord ratio the values of z_w decrease, but the experimental results were not conclusive in this range.

8. References

1. A.L. Buchan, K.D. Harris, P.M. Somervail. Measurement of the derivative z_w for an oscillating aerofoil. College of Aeronautics Rep. No. 40 (1950).

2. B.S. Campion, E.G. Scacy. Measurement of the derivative z_w for oscillating wings in cascade. Report on experimental work done at C. of A. (1953). Unpublished.

3. G.E. Whitmarsh. Measurement of the derivative z_w for oscillating sweptback wings. College of Aeronautics Rep. No. 92, 1955.

4. H.A. Simon, F.E. Bartholomew. Measurement of the damping derivative z_w for swept-back wings. Report on experimental work done at C.of A. (1951). Unpublished.

References (Contd.)

5. W. P. Jones — Theoretical Air-load and Derivatives Coefficients for Rectangular Wings. A.R.C. R. and M. No. 2142.

6. G. M. Lilley — An investigation of the Flexure-Torsion flutter characteristics of aerofoils in cascade. College of Aeronautics Rep. No. 60, 1952.

7. D.S. Woolston, H.L. Runyan — Some considerations on the air forces on a wing oscillating between two walls for subsonic compressible flow. Jnl. Aero. Scs. Vol. 22, 1955, pp.41-50.

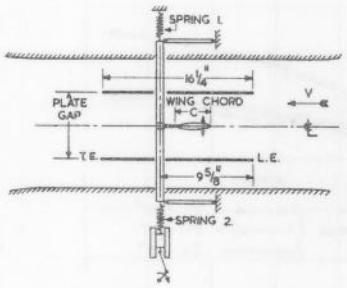

POSITION OF PLATES IN TUNNEL.

FOR FURTHER DETAILS OF RIG SEE REF 1.

FIG. 1.

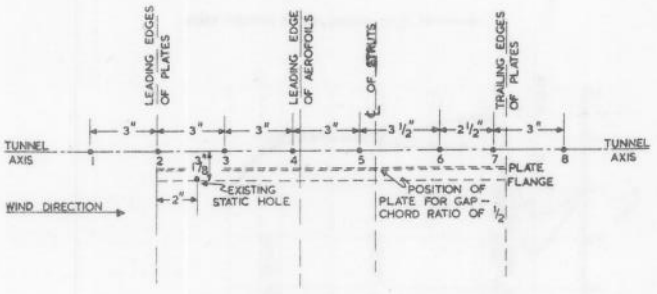

POSITION OF STATIC HOLES IN ROOF OF TUNNEL.

FIG. 4.

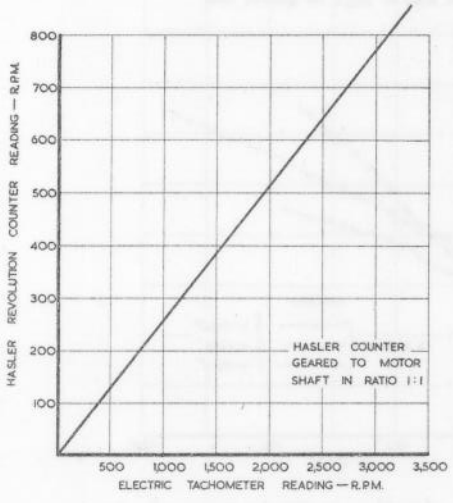

CALIBRATION OF ELECTRIC TACHOMETER AGAINST HASLER COUNTER.

FIG. 2.

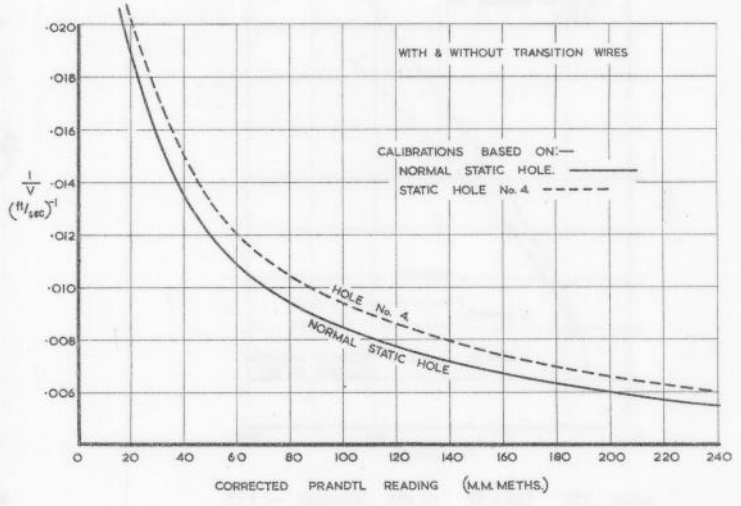

PLATE SPACING — 1/2 C

FREESTREAM WINDSPEED BETWEEN PLATES AT MODEL POSITION.

FIG. 5.

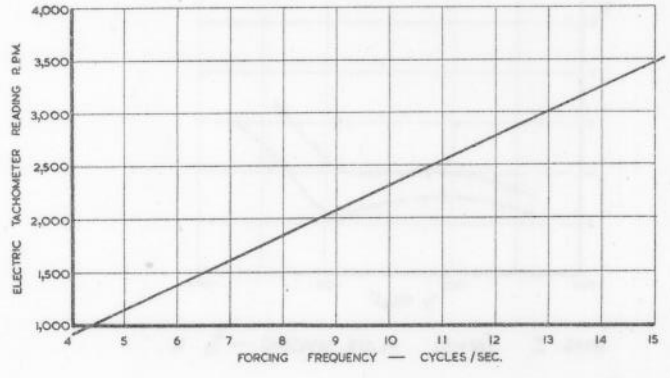

FREQUENCY OF OSCILLATION AGAINST ELECTRIC TACHOMETER READING.

FIG. 3.

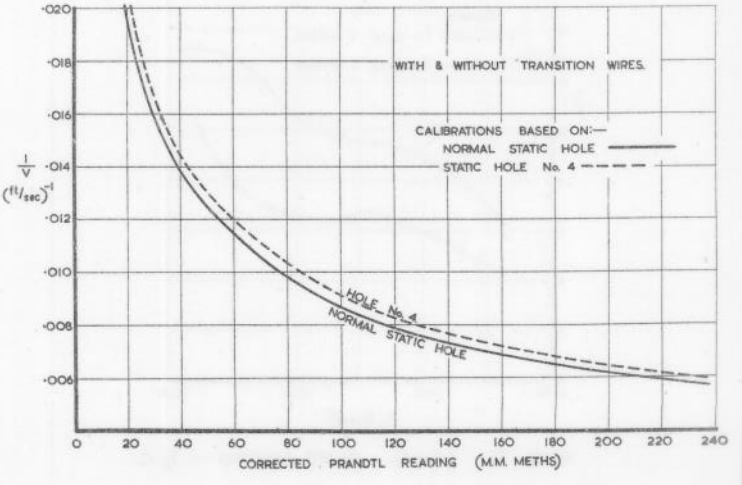

PLATE SPACING — 1/3 C

FREESTREAM WINDSPEED BETWEEN PLATES AT MODEL POSITION.

FIG. 6.

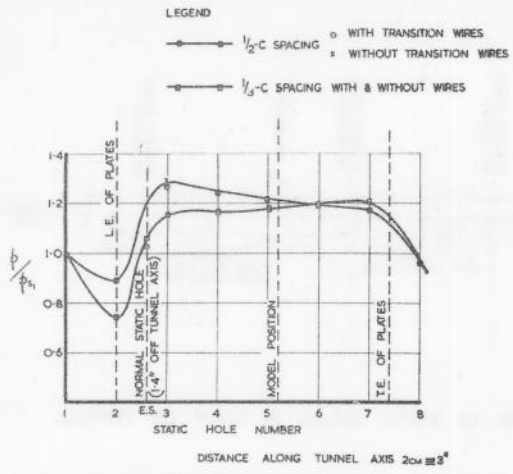

RATIO OF STATIC PRESSURES AT HOLES ALONG TUNNEL AXIS TO THAT AT HOLE No. 1.

FIG. 7

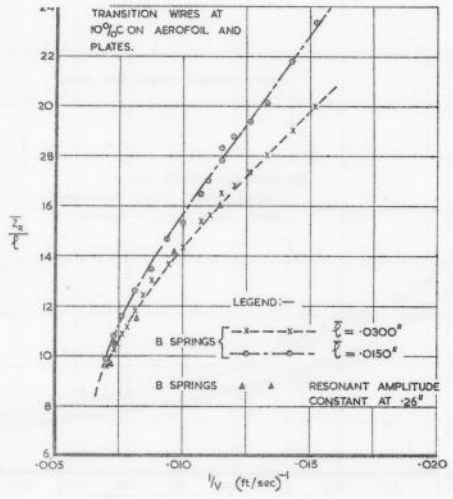

WING III (AR=3) PLATE SPACING — 1 C.

FIG. 8.

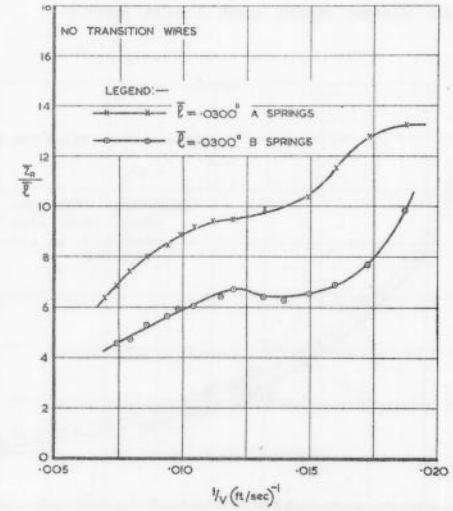

WING II (AR=4) PLATE SPACING — ½ C.

FIG. 9.

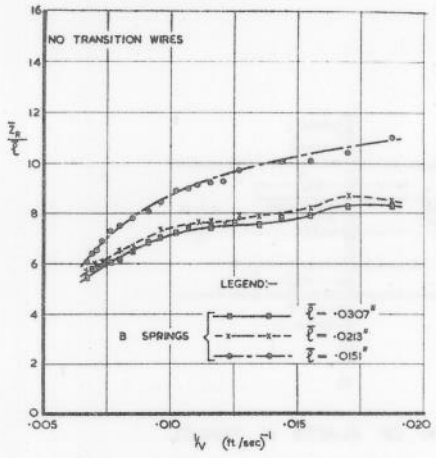

WING III (AR=3) PLATE SPACING — ½ C.

FIG. 10.

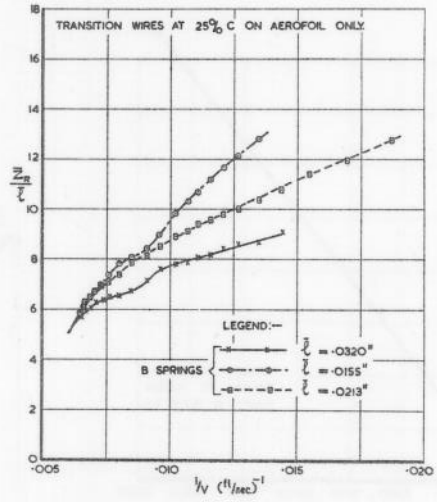

WING III (AR=3) PLATE SPACING — ½ C.

FIG. 11.

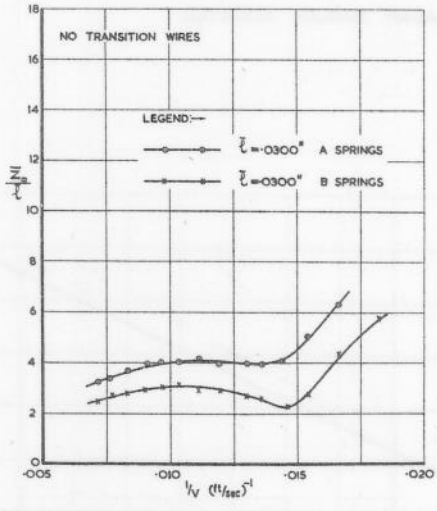

WING. I (AR=5) PLATE SPACING — ⅓ C.

FIG. 12.

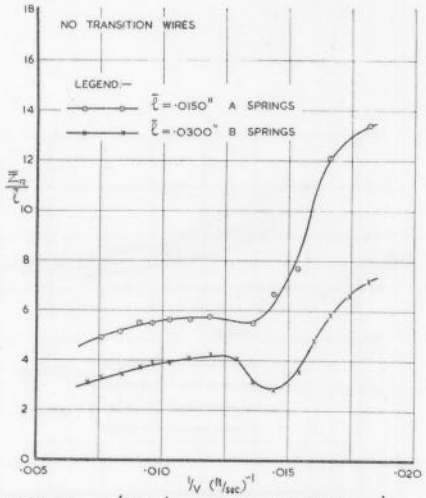

WING. II (AR=4) PLATE SPACING — 1/3 C.

FIG. 13.

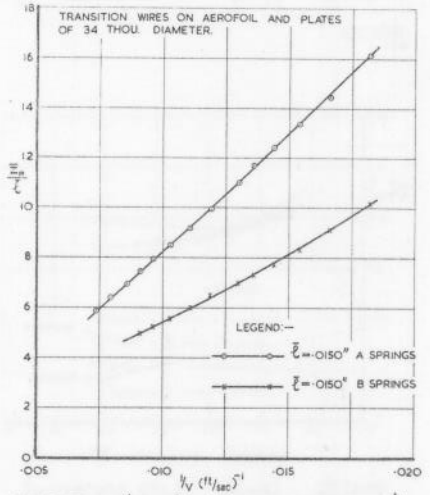

WING II (AR=4) PLATE SPACING — 1/3 C.

FIG. 14.

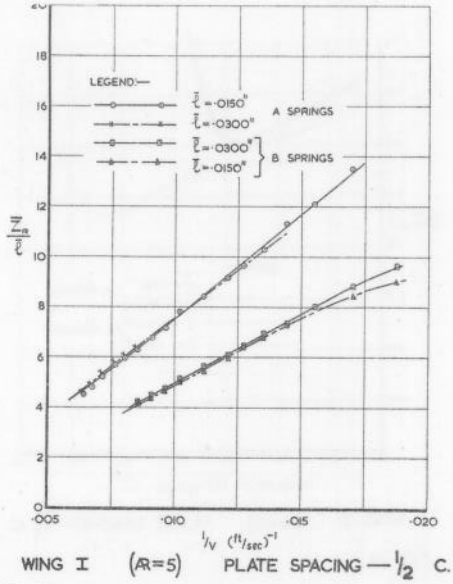

WING I (AR=5) PLATE SPACING — 1/2 C.

FIG. 15.

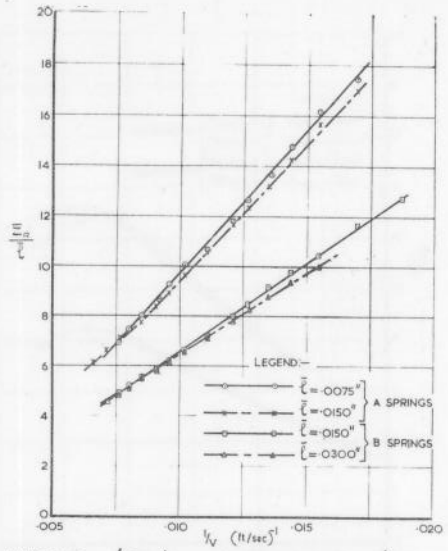

WING II (AR=4) PLATE SPACING — 1/2 C.

FIG. 16.

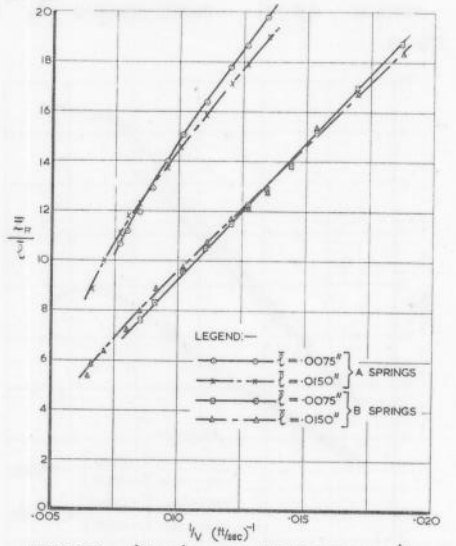

WING III (AR=3) PLATE SPACING — 1/2 C.

FIG. 17.

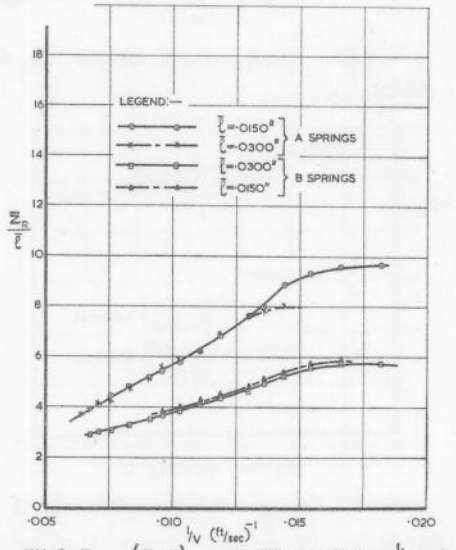

WING I (AR=5) PLATE SPACING — 1/3 C.

FIG. 18.

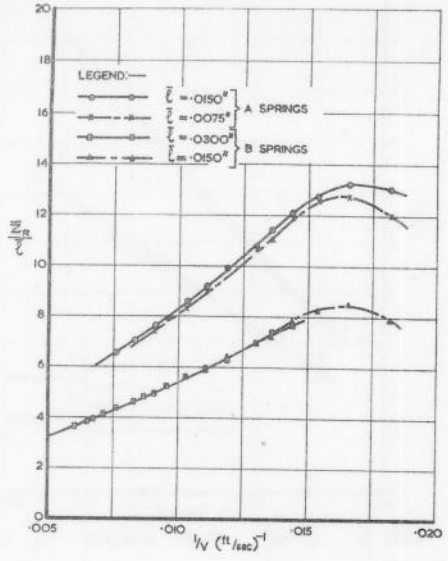

WING II (AR=4) PLATE SPACING — 1/3 C.

FIG. 19.

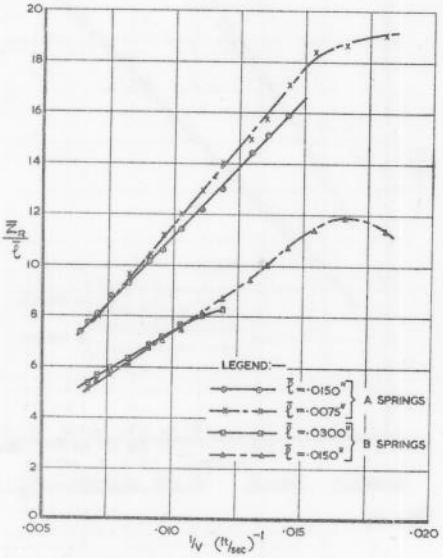

WING III (AR=3) PLATE SPACING — 1/3 C.

FIG. 20.

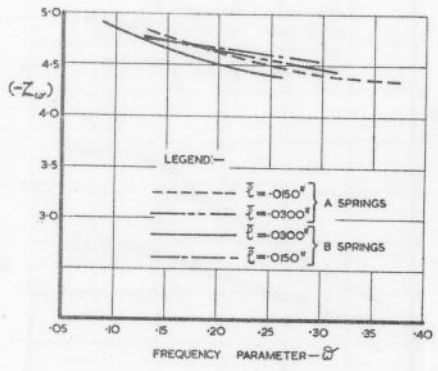

WING I (AR=5) PLATE SPACING — 1/2 C.

FIG. 21.

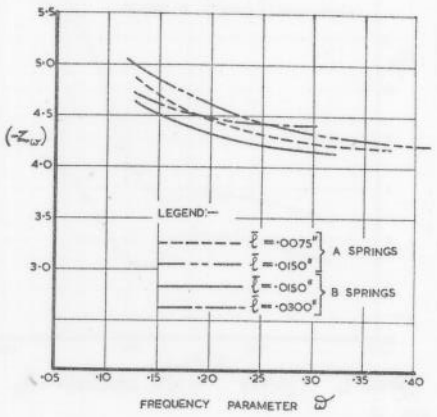

WING II (AR=4) PLATE SPACING — 1/2 C.

FIG. 22.

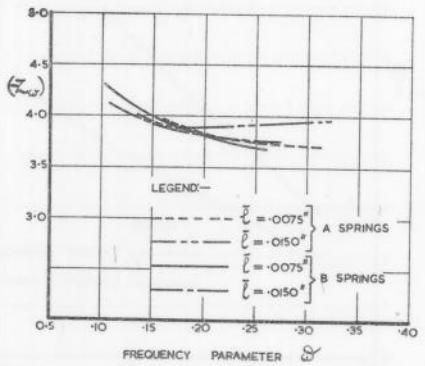

WING III (AR=3) PLATE SPACING — 1/2 C.

FIG. 23.

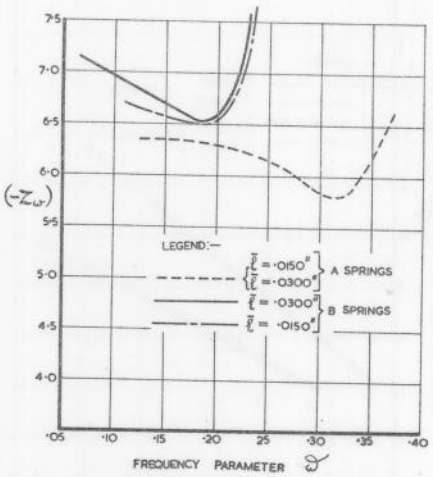

WING I (AR=5) PLATE SPACING — 1/3 C.

FIG. 24.

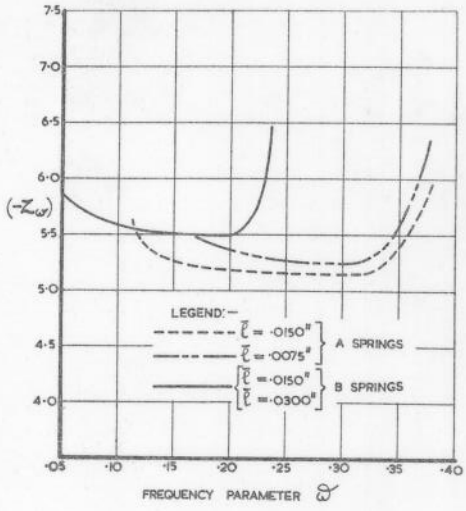

WING II $(AR=4)$ PLATE SPACING — $1/3$ C.

FIG. 25.

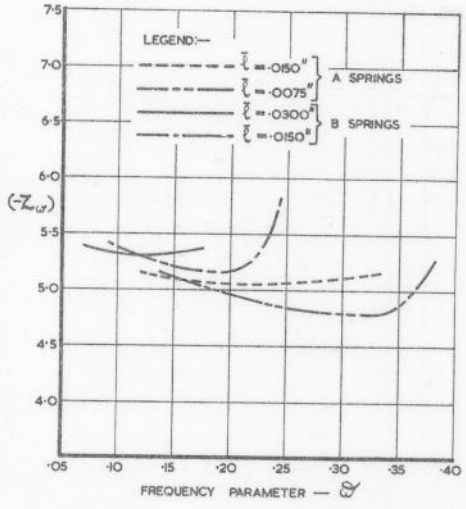

WING III $(AR=3)$ PLATE SPACING — $1/3$ C.

FIG. 26.

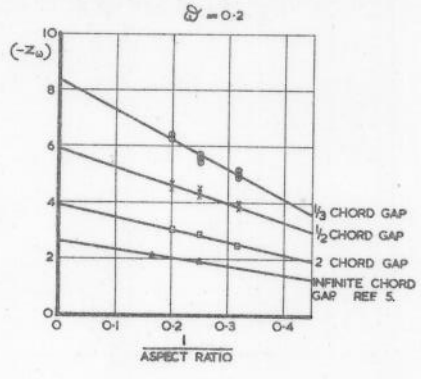

EXPERIMENTAL RESULTS FOR $Z_{w\sigma}$ EXTRAPOLATED TO GIVE VALUES OF $Z_{w\sigma}$ AT INFINITE ASPECT RATIO.

FIG. 27.

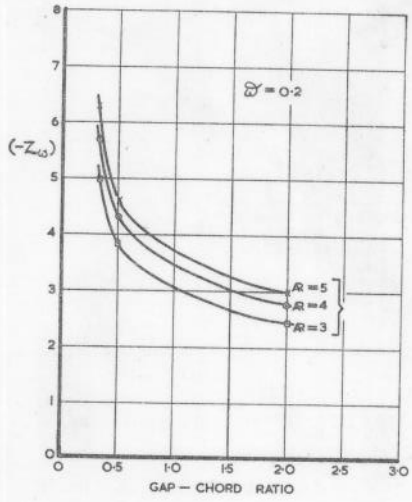

EXPERIMENTAL VALUES OF $Z_{w\sigma}$ FOR VARYING GAP—CHORD RATIO.

FIG. 28.

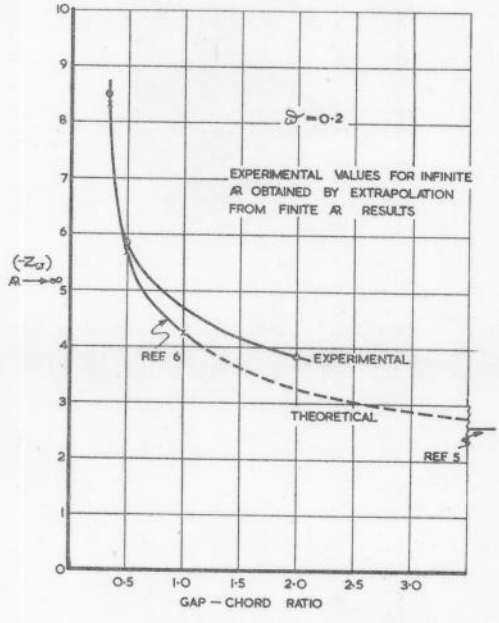

COMPARISON OF THEORETICAL AND EXPERIMENTAL VALUES OF $Z_{w\sigma}$ FOR INFINITE ASPECT RATIO.

FIG. 29.